Exciton dynamics for extended monolayer islands in thin $In_{0.53}Ga_{0.47}As/InP$ quantum wells

G. Bacher, J. Kovac, K. Streubel, H. Schweizer, and F. Scholz
4 Physikalisches Institut, Universität Stuttgart, Pfaffenwaldring 57, D-7000 Stuttgart 80, Federal Republic of Germany
(Received 20 November 1991)

The exciton dynamics for extended monolayer islands in thin growth-interrupted $In_{0.53}Ga_{0.47}As/InP$ quantum wells is investigated with use of temperature-dependent and time-resolved photoluminescence spectroscopy. Three different temperature regimes are found. At temperatures below 40 K, no coupling between neighboring islands is observed, indicating exciton localization at potential fluctuations at the interface. Increasing the temperature causes exciton delocalization and the decay of excitonic luminescence is influenced by the exciton transfer between the islands. At temperatures above 130 K, the islands are strongly coupled and the transfer occurs within our time resolution of about 50 ps. A model is developed to describe the exciton transfer quantitatively. We are thus able to determine the exciton mobility to values up to 150 $cm^2/V\,s$ for an effective well width of 2 monolayers ($\simeq 0.6$ nm). Analyzing our experimental results theoretically, we conclude that, at low temperatures, inelastic scattering—and, therefore, exciton localization—is dominant. This result is confirmed by the nearly temperature-independent excitonic lifetime in this temperature region. At higher temperatures, however, the excitons become delocalized and we show, by comparison with theory, that the mobility is controlled by interface roughness scattering.

I. INTRODUCTION

The interface morphology in semiconductor heterostructures is of great interest, especially for the performance of high-mobility transistors. It has been shown theoretically[1,2] and experimentally[2,3], that interface roughness scattering (IRS) can be the dominant scattering process limiting the carrier mobility in thin quantum wells. At low temperatures, the excitons may even be localized at potential fluctuations caused by the interface roughness.[4,5] On the other hand, the properties of the quantum-well luminescence are also influenced by the interface structure. A shift between the emission line and the absorption peak, the so-called "Stokes shift"[5] as well as a broadening of the photoluminescence (PL) linewidth[5,6] is caused by a certain roughness of the interface. Improvement of the interface quality should not only increase the mobility but also reduce the luminescence linewidth.

Extensive studies have been performed to optimize the epitaxial growth process with respect to the interface quality in quantum-well structures. The interruption of growth at the heterointerfaces has been found to be a powerful method for a smoothing of the interfaces in molecular-beam epitaxy[3,7–9] and in metalorganic vapor-phase epitaxy (MOVPE).[10–14] In such structures two or even more sharp emission peaks can be observed from a single quantum well in the $GaAs/Al_xGa_{1-x}As$ as well as in the $In_{1-y}Ga_yAs/InP$ system. This is attributed to excitonic recombination in different areas of the quantum well, where the effective well width differs by one atomic monolayer (ML). Hence, the lateral size of these islands must be larger than the exciton diameter. Using cathodoluminescence measurements, extended monolayer flat islands (extensions up to several μm) have been observed in both, the $GaAs/Al_xGa_{1-x}As$ (Ref. 15) and the $In_{1-y}Ga_yAs/InP$ (Refs. 16 and 17) system.

Several experiments concerning the carrier dynamics in such a system have been performed in $GaAs/Al_xGa_{1-x}As$ quantum wells.[18–21] The transfer of carriers between neighboring island regions was studied by means of time-resolved PL spectroscopy. The difference in the measured transfer times has been explained by the difference in the well width and the island geometry of the samples. To study the improvement of the interface quality due to growth interruption (GRI) in this material system, a set of transport measurements using time- and spatially resolved spectroscopy has been performed.[3] An increase of the carrier mobility due to reduced IRS was found in samples with GRI at both interfaces.

On the other hand, no systematic study of the carrier dynamics in GRI $In_{1-y}Ga_yAs/InP$ quantum wells has been published up to now. Recent publications[22,23] only demonstrate the carrier transfer between extended islands using temperature-dependent PL spectroscopy.

In this paper, we present a systematic study of the exciton dynamics in $In_{1-y}Ga_yAs/InP$ quantum wells which have been grown by low-pressure MOVPE with GRI at each interface. We performed temperature-dependent and time-resolved experiments to investigate quantitatively the transfer between extended monolayer flat islands. A theoretical model including the diffusion in the islands and the interaction of different island regions is presented. The quantitative analysis of our experimental results is used to identify the dominant scattering process, i.e., IRS, limiting the exciton mobility in the islands and therefore controlling the effective transfer time be-

tween different island regions. Furthermore, we demonstrate the influence of exciton localization on the exciton dynamics, especially on the lifetime and on the mobility.

The paper is organized as follows. In Sec. II, we describe the experimental setup and the sample characterization. In Sec. III, time-resolved experiments using picosecond spectroscopy are presented. A model describing the carrier transfer is developed in Sec. IV and the temperature dependence of the exciton diffusion is discussed. For a comparison with calculations of the ambipolar mobility including IRS and alloy scattering (AS), we additionally analyze the PL linewidth to get more information about the interface morphology. The paper concludes with a short summary of our results.

II. EXPERIMENTAL SETUP AND SAMPLE CHARACTERIZATION

The $In_{0.53}Ga_{0.47}As/InP$ quantum-well structure under investigation was grown by low-pressure MOVPE using GRI at each interface to improve the interface quality. The sample consists of four quantum wells with different nominal well widths ($\langle L_z \rangle = 0.7$, 1.5, 3, and 10 nm) separated by a 100-nm-thick InP barrier to avoid quantum-mechanical coupling between the wells. At the bottom ($In_{1-y}Ga_yAs$ on InP) interface the growth was interrupted for 1 s by switching the In and P precursor flow from the run line to the vent line, while AsH_3 was used to stabilize the surface. The other (InP on $In_{1-y}Ga_yAs$) interface was interrupted for 2×7.5 s. First, the reactor was flushed with pure H_2. Then PH_3 was switched to the reactor in order to prepare the growth of the following InP layer. Further details concerning the optimization of the growth process are already published.[24]

In the experiments presented in this paper, the sample temperature was varied between 2 and 300 K in a He-bath cryostat. Time-integrated measurements were performed using the 514.5-nm line of an Ar^+-ion laser for the sample excitation and a Ge detector and a lock-in amplifier for the detection of the luminescence signal. As excitation source for the time-resolved experiments, a synchronously mode-locked (DCM) [4-(dicyanomethylene)-2-methyl-6-(p-dimethylaminostyryl)-4*H*-pyran] dye laser pumped by an actively mode-locked Ar^+-ion laser was used. Detection of the decaying PL was obtained by a fast microchannel plate photomultiplier with *S*1 response. The laser pulse width of 10 ps results in an overall time resolution of about 50 ps. The intensity and the focus of the exciting laser spot were adjusted to keep a carrier density of about 5×10^9 cm^{-2} in the wells. In this density region, the excitonic luminescence dominates the radiative recombination in the quantum wells.

In Fig. 1, a part of the luminescence spectrum of the sample at different temperatures is depicted. The emission of the quantum wells with the nominal thickness of $\langle L_z \rangle = 0.7$, 1.5, and 3 nm, respectively, consists of two or

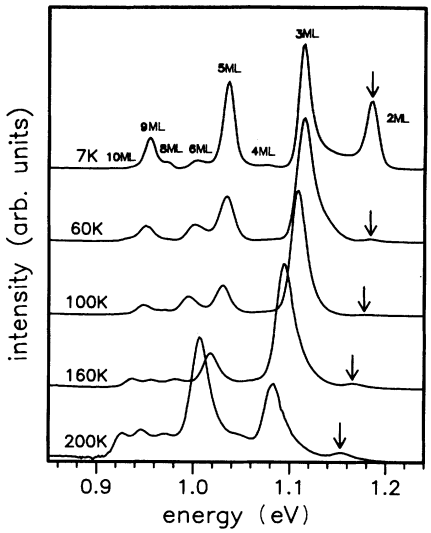

FIG. 1. Photoluminescence spectra of an $In_{0.53}Ga_{0.47}As/InP$ multiple quantum-well structure for various temperatures. The nominal thicknesses are 0.7, 1.5, 3, and 10 nm (not plotted here). The spectral position of the 2-ML peak is indicated by an arrow. Note the monolayer splitting of the quantum-well emission.

three well-resolved peaks, indicating the existence of extended monolayer islands with effective well widths separated by one atomic monolayer (1 ML $\cong$0.283 nm). The low-temperature ($T=7$ K) luminescence linewidths of 15.5 and 14.7 meV for the 2- and 3-ML peaks, respectively, gives evidence of an excellent sample quality and very good heterostructure interfaces. As can be seen in the following, a variety of information can be extracted from this temperature series.

Due to the thermal coupling between the islands, the intensity ratio of different regions changes with temperature. For a detailed discussion, let us first focus on the thinnest quantum well with the nominal width of 0.7 nm (2- and 3-ML peaks, see Fig. 1).

At 7 K, the intensity of the 2-ML regions is about half the value of the intensity of the 3-ML regions. Increasing the temperature reduces the 2-ML intensity, while the intensity of the 3-ML islands grows, indicating an effective carrier transfer between the different regions. Thermal occupation of the 2-ML regions results in another increase of the 2-ML intensity at temperatures of about 160 K. A further rise of the bath temperature to values larger than 200 K induces a drastic drop of the intensity of this quantum well. This can be explained by the thermal emission of the carriers into the InP barrier followed by a capture in neighboring quantum wells or nonradiative recombination at the sample surface or in the substrate, respectively.[25]

The temperature dependencies of the other quantum wells can be discussed in a similar manner. Hence, the thermal behavior and the energetic position of the PL peaks enables us to identify the quantum wells belonging to the emission peaks.

III. EXPERIMENTAL: TIME-RESOLVED SPECTROSCOPY

For a detailed investigation of the exciton dynamics, we will focus on the quantum well with the nominal thickness of 0.7 nm. As mentioned above, the quantum-well emission consists of two main peaks corresponding to an effective well width of 2 and 3 ML, respectively. The spectra presented in Fig. 1 indicate that the intensity ratio not only reflects the ratio of the 2- and 3-ML island areas, but also the interaction between different islands. For a detailed and quantitative understanding of the transfer dynamics between the islands, time-resolved experiments are necessary.

In Fig. 2, transient spectra of this quantum well for two different temperatures are plotted. At $T=13$ K (left-hand side of Fig. 2), the intensity ratio between the 2- and 3-ML peaks is nearly constant within their lifetime. The small difference in the luminescence decay occurs from the slightly different excitonic lifetimes in both regions (see Fig. 3). We conclude that there is no transfer between the different regions at low temperatures. This means a diffusion length of the excitons smaller than the extension of the monolayer islands. The ratio of the island areas determines the intensity ratio and is found to be $A_{2\,\mathrm{ML}}/A_{3\,\mathrm{ML}} \simeq 1/2$.

On the other hand, a distinct variation of the intensity ratio with increasing time is found at $T=50$ K (right-hand part of Fig. 2). The emission intensity of the 2-ML regions vanishes after several hundreds of ps. Simultaneously, an increase of the intensity of the 3-ML peak is observed, indicating an effective carrier transfer between the islands.

To demonstrate the variation of the luminescence decay with temperature, we have plotted the peak intensity of the two different island regions as a function of time for different temperatures (Fig. 3). At low temperature ($T=15$ K), where no transfer occurs (see Fig. 2), excitonic recombination dominates the luminescence decay. As

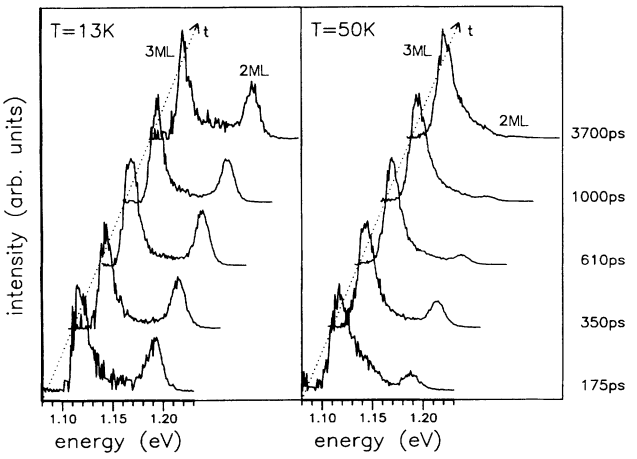

FIG. 2. Transient emission spectra of one well (nominal well width 0.7 nm) indicating exciton localization ($T=13$ K; to the left) and exciton transfer ($T=50$ K; to the right) between the extended islands.

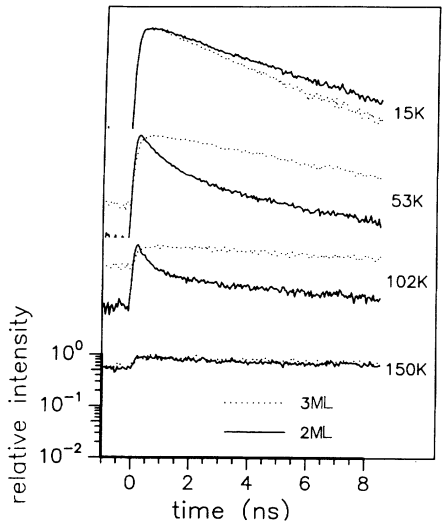

FIG. 3. Decay of the excitonic luminescence of the 2- and the 3-ML regions in the well with $\langle L_z \rangle = 0.7$ nm. Note the variation of the exciton dynamics with increasing temperature.

the intrinsic lifetime depends on the effective well width,[26,27] an enlarged decay time of the 2-ML regions with respect to the 3-ML regions is observed. The difference of about 20% is in good agreement with the results given in Ref. 27.

Increasing the temperature changes the behavior of the luminescence decay in the different regions. While the lifetime of the excitons in the 3-ML islands increases, we observe a nonexponential decay in the 2-ML islands. The fast decay at the beginning arises from the carrier transfer to the regions with an effective well width of 3 ML. Simultaneously, a delayed offset of the luminescence signal from the 3-ML regions due to the exciton transfer is found. An analysis of this behavior yields information about the dynamics o f the carrier transfer between the islands. If the thermal equilibrium between the different islands is established, the decay time is given by the excitonic lifetime in the thermally coupled system of 2–3-ML regions.

At 150 K, no difference in the time behavior of the two regions can be observed. The thermal equilibrium is achieved within our time resolution of 50 ps and the whole system reveals a monoexponential decay.

Before analyzing the exciton transfer, we will discuss the temperature dependence of the excitonic lifetime in our sample. The decay time of the 3-ML region, which is not strongly influenced by the transfer, is depicted versus temperature (Fig. 4). A monoexponential decay with lifetimes up to 35 ns indicates the excellent sample quality. As already observed in $GaAs/Al_xGa_{1-x}As$ quantum wells,[28,29] three different temperature ranges can be discussed.

(i) At low temperatures, the measured lifetime is nearly independent of temperature. Spatial fluctuations of the well width or the alloy composition cause a variation of the potential, where the excitons can be localized.[4,5] For free excitons, a temperature dependence according to

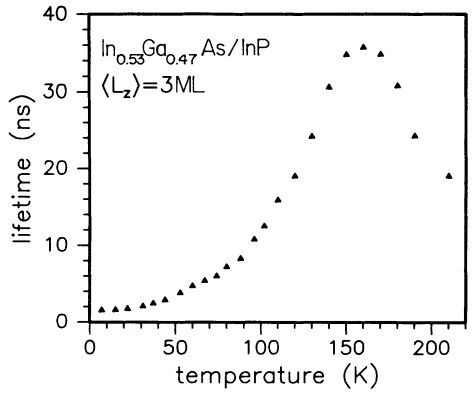

FIG. 4. Excitonic lifetime of the 3-ML regions vs bath temperature.

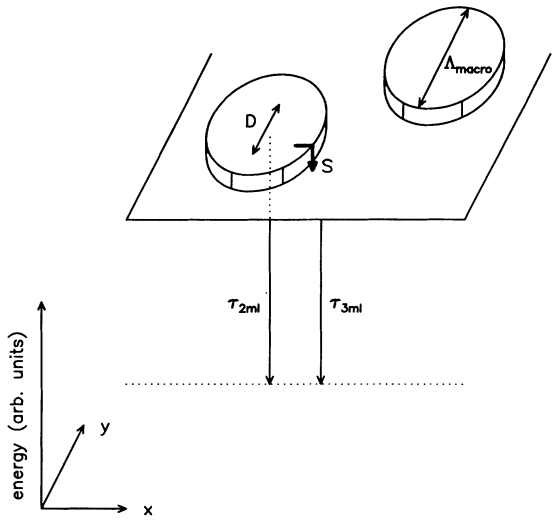

FIG. 5. Schematic diagram of the scenario used in the transfer model as described in the text.

$\tau(T) \propto \Delta_h(T)\{1-\exp[-\Delta_h(T)/k_B T]\}^{-1}$ is expected[26] [$\Delta_h(T)$ denotes the homogeneous excitonic linewidth]. In this case, the thermal distribution of the excitons in **k** space reduces the transition probability with increasing temperature. However, it is not possible to fit our experimental values according to this theory. On the other hand, localized excitons have a negligible kinetic energy compared with free excitons, resulting in a temperature-independent transition probability. The dominance of localized excitons at low temperatures is in agreement with the extremely low mobilities in this temperature regime determined in this quantum well (see Sec. IV).

(ii) Increasing the temperature to values above 50 K delocalizes the excitons and more and more excitons can take up kinetic energy. We observe a distinct increase of the luminescence lifetime as expected for delocalized excitons.

(iii) At temperatures larger than 160 K, the lifetime decreases drastically. In agreement with recent experiments in shallow $In_xGa_{1-x}As/GaAs$ quantum wells,[25] the decay time as well as the luminescence intensity (see Fig. 1) is reduced due to the thermal emission of the carriers into the barrier.

IV. ANALYSIS OF THE EXCITON TRANSFER

The experiments presented above have shown that the exciton transfer between the islands occurs at temperatures higher than 50 K. For a quantitative description of the exciton dynamics, we have developed a model including the excitonic diffusion in the islands and a transfer velocity S at the border of the islands. Figure 5 schematically demonstrates the scenario assumed in our model. In the energy range of the 0.7-nm quantum well (1.1–1.2 eV at 7 K), the PL spectra (see Fig. 1) consist of two main peaks, indicating the existence of extended islands mainly at one interface, while the morphology of the other is probably determined by some microroughness (i.e., islands with a typical extension smaller than the exciton diameter). In a first approximation, we describe the islands with high energy emission, i.e., the 2-ML regions, as a cylinder with diameter Λ_{macro} and height Δ ($\Delta = 1$ ML). The step height of 1 ML corresponds in this quantum well to an energetic difference of 70 meV (see Fig. 1). Within their lifetime the carriers are able to diffuse to the border of the islands and can be scattered to the lower-energy islands (3-ML regions) with a transfer velocity S. According to the findings in the time-resolved experiments, a monoexponential decay with the characteristic time constants $\tau_{2\,\mathrm{ML}}$ and $\tau_{3\,\mathrm{ML}}$, respectively, is used in our model.

The carrier concentration $c_{2\,\mathrm{ML}}(r,t)$ in the 2-ML regions is reduced due to the finite recombination lifetime and additionally due to the transfer into the 3-ML regions and can be described by the following equation:

$$\frac{\partial c_{2\,\mathrm{ML}}(r,t)}{\partial t} = -\frac{c_{2\,\mathrm{ML}}(r,t)}{\tau_{2\,\mathrm{ML}}} + D\,\Delta c_{2\,\mathrm{ML}}(r,t) \tag{1}$$

including the surface condition

$$-\frac{\partial c_{2\,\mathrm{ML}}(r,t)}{\partial t}\bigg|_{r=\Lambda_{\mathrm{macro}}/2} = S[c_{2\,\mathrm{ML}}(r=\Lambda_{\mathrm{macro}}/2,t) - c_{2\,\mathrm{ML}}(r=\Lambda_{\mathrm{macro}}/2,\ t=\infty)]\ . \tag{2}$$

D corresponds to the excitonic diffusion constant, $\tau_{2\,\mathrm{ML}}$ is the carrier lifetime in the 2-ML region, and S is the transfer velocity at the border of the 2-ML islands. For $t \to \infty$, thermal equilibrium between the different islands is achieved.

Integration over the island area gives the total carrier population in the 2-ML regions. Using the solution of this problem, it is possible to calculate the transfer-induced variation of the carrier population in the 3-ML regions. The transient intensity depends on the lifetimes $\tau_{2\,\mathrm{ML}}$ and $\tau_{3\,\mathrm{ML}}$, respectively, and on the carrier transfer between the islands. The transfer is mainly determined by the diffusion constant D, the transfer velocity S, and

the averaged island extension Λ_{macro} of the 2-ML regions. The details of the model and the solution are further explained in the Appendix.

For an estimation of the value of S, we refer to calculations of Kuhn and Mahler.[30] They developed a surface model for ambipolar transport in a hydrodynamic theory. Neglecting the carrier reflection at the surface, they get $S=[k_B T/(2\pi m)]^{0.5}$, where k_B is the Boltzmann constant and m the effective mass of the carrier. In our case, this corresponds to values $S > 10^6$ cm/s. Using the values of the island extension Λ_{macro} and of the diffusion constant D (see below), we get $L=\Lambda_{\text{macro}} S/2D \gg 1$. Hence, the transfer is limited by the carrier diffusion in the islands, whereas the exact value of S does not influence the dynamics significantly.

Figure 6 demonstrates the validity of our model. As explained above (see Figs. 2 and 3), the exciton transfer modifies the luminescence decay in this temperature region ($T=53$ K). The intensity decay of both the 2- and 3-ML regions is fitted by the model discussed above. On the one hand, the transfer shortens the characteristic decay of the 2-ML emission, and on the other hand, the onset of the intensity of the 3-ML regions is modified.

Most of the parameters used in our model can be extracted from our experiments. The lifetime $\tau_{3\text{ ML}}$ can be extracted by the monoexponential decay of the 3-ML intensity. According to the excitonic lifetime at low temperatures (see Fig. 3), the temperature-dependent carrier lifetime in the 2-ML regions is assumed to be about 20% higher than in the 3-ML regions. The ratio $A_{2\text{ ML}}/A_{3\text{ ML}}$ of the island regions is given by the low-temperature spectrum, where the transfer can be neglected. Therefore, in the case of $L \gg 1$, the only fit parameter used to describe the time dependence of the luminescence intensity of both regions is $D/\Lambda^2_{\text{macro}}$.

For an analysis of the dominant scattering processes limiting the transfer dynamics, a discussion of the temperature dependence of the exciton mobility is necessary. An extraction of the diffusivity from our experiments is only possible with the knowledge of the extension Λ_{macro} of the monolayer islands. Cathodoluminescence measurements performed by Grundmann *et al.*[31] on this sample, give an estimation for the average island diameter in the range of 1 μm. With this information, we are able to calculate the diffusion constant and by using the Einstein relation we get the exciton mobility as a function of temperature.

The result is plotted in Fig. 7. Two different temperature regions are found. At low temperatures, we observe a strong increase of the mobility with increasing temperature. The main scattering processes in this low-temperature regime should be AS, IRS, and impurity scattering (IMS). Neglecting screening, AS and IRS are nearly independent of temperature in this temperature region.[1,2] On the other hand, we expect a linear increase of the mobility with temperature in the case of IMS.[32] However, the result of our experiments is very different from these behaviors. Hence, we conclude that exciton localization dominates the carrier dynamics at low temperatures, reducing the exciton mobility drastically. This was also assumed by Hillmer *et al.*[28] for the $GaAs/Al_xGa_{1-x}As$ system. The exciton localization is caused by inelastic scattering and cannot be described by an elastic scattering theory. The appearance of exciton localization in $In_{1-y}Ga_yAs/InP$ quantum wells at low temperatures was also found by Hegarty, Tai, and Tsang,[4] in agreement with our interpretation.

At temperatures between 60 and 130 K, the measured exciton mobility is nearly independent of temperature. Phonon scattering would cause a reduction of the mobility with increasing temperature, in contradiction to this result. Hence, two other scattering processes are possible to explain the experimental findings: AS and IRS.

We have calculated AS in this quantum well using the theory given by Brum and Bastard[33] and have found an ambipolar mobility which is indeed independent of temperature, but orders or magnitude larger than our experimental values. In this thin quantum well, the main part of the wave function spreads out into the barrier, reducing the influence of AS drastically.

Hence, IRS is the dominant scattering process controlling the exciton transfer between extended monolayer is-

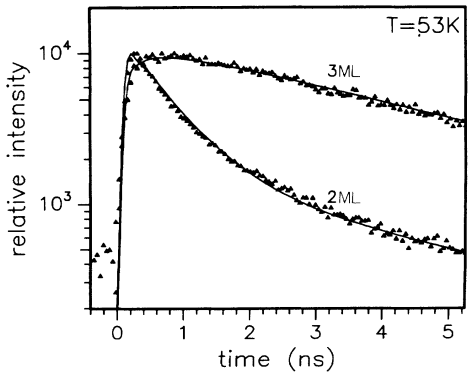

FIG. 6. Luminescence intensity as a function of time for the 2- and 3-ML regions, respectively (experiment: symbols) including a fit with the model presented in the text (solid line).

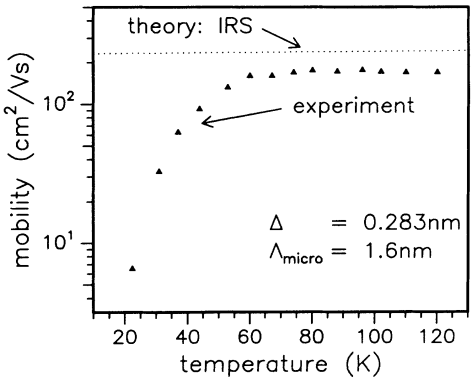

FIG. 7. The exciton mobility vs temperature as extracted from the experiment (symbols) assuming an extension of the macroislands $\Lambda_{\text{macro}} \cong 1$ μm in comparison to the theory of interface roughness scattering (dotted line). In the theory, a microroughness of $\Lambda_{\text{micro}} \cong 1.6$ nm is assumed according to the analysis of the PL linewidth.

lands in the temperature regime between 60 and 130 K. To calculate the influence of IRS, we need more information about the interface morphology.

For a moment, let us refer to the GaAs/$Ga_xAl_{1-x}As$ system. In the past, a detailed discussion concerning the interface morphology, especially the observation of some microroughness in growth-interrupted quantum wells, arose.[34,35] The monolayer splitting of the quantum-well emission indicates the existence of macroislands with diameters larger than the exciton extension. On the other hand, high-resolution transmission electron microscopy (HRTEM) measurements manifested some "microroughness" with an extension of only a few nanometers at the interfaces.[36]

We now return to the low-pressure MOVPE-grown $In_{0.53}Ga_{0.47}As$/InP material. If in our sample both interfaces were atomically smooth, consisting only of macroislands with $\Lambda_{macro} \cong 1$ μm as observed by the cathodoluminescence measurements, the excitonic linewidth should be quite narrower (the influence of fluctuations in the alloy can be neglected in such narrow quantum wells; see the discussion below) and the mobility orders of magnitude larger than observed in our experiments. Hence, we have to take into account some microroughness controlling the emission linewidth and the exciton mobility in our structure. However, it is not possible to decide whether the microroughness occurs only at one or at both interfaces. So, additional HRTEM measurements have been performed at a comparable sample.[24] Based on these results, we assume a similar microroughness at both interfaces.

Variable growth conditions (GRI at either the bottom—$In_{1-y}Ga_yAs$ on InP—or the top—InP on $In_{1-y}Ga_yAs$—interface) are used for a further analysis of the interface structure. If the quantum wells are grown without GRI after the InP layer, a monolayer splitting is still observed. On the contrary, the line splitting disappears if no GRI is used after the growth of $In_{1-y}Ga_yAs$. So the formation of growth islands only at the top interface seems to be likely, in agreement with the observation of two main peaks in the PL spectrum of each quantum well. As proposed by Warwick, Jan, and Ourmazd[37] for GaAs/$Al_xGa_{1-x}As$, the interface roughness spectrum of the top interface seems to be "bimodal," on the one hand, extended islands and on the other hand, a certain microroughness, while only a microroughness forms the morphology of the bottom interface.

A method to get more quantitative information about the microroughness is the analysis of the luminescence linewidth. The measured exciton linewidth of the 2-ML region was about 15.5 meV. In thin undoped $In_{1-y}Ga_yAs$/InP quantum wells, two main broadening effects are expected: interface roughness and local fluctuations of the composition. An estimation of the influence of the alloy broadening according to the theory of Sugawara *et al.*[38] shows the negligible contribution of alloy broadening in $In_{1-y}Ga_yAs$/InP quantum wells with well widths less than 1 nm.

The microroughness of the heterointerfaces can be described by a step height Δ and a lateral size Λ_{micro}. A quantitative calculation of the linewidth broadening according to the interface roughness is given by Singh, Bajaj, and Chandhuri.[6] The broadening is mainly determined by the ratio of the exciton extension, which is twice the exciton radius, and the island diameter. Taking into account a step height Δ of one monolayer (0.283 nm) and an expectation value of the exciton radius of 16 nm for $L_z = 2$ ML,[39] the experimental linewidth of 15.5 meV can be explained by a lateral size $\Lambda_{micro} \cong 1.6$ nm of the microislands. In this calculation, a comparable microroughness at both interfaces was assumed, according to the discussion above.

Now, knowing the interface morphology, we resume the discussion of the exciton mobility. To calculate the temperature dependence of IRS, we apply the theory of Sakaki *et al.*[2] and additionally, we take into account the finite barrier height of the potential well. The mobility is controlled by the carrier density and the step height Δ and the lateral step size Λ_{micro} of the microislands.

The carrier density was estimated from the exciting power density and the absorption coefficient of InP to be about 5×10^9 cm^{-2} in the well. In this density region, screening can be neglected and the mobility controlled by the microroughness is nearly independent of the carrier density.

The effective mass for the electron and the hole, respectively, is calculated taking into account the extension of the wave functions into the barrier, but neglecting the nonparabolicity of the valence band,

$$m_{i\parallel} = m_{i\parallel}^{QW} \langle \Psi_i | \Psi_i \rangle_{QW} + m_{i\parallel}^{b} \langle \Psi_i | \Psi_i \rangle_b \ . \tag{3}$$

The probability of finding the carrier i ($i = e, hh$) in the quantum well (in the barrier) is given by the expression $\langle \Psi_i | \Psi_i \rangle_{QW}$ ($\langle \Psi_i | \Psi_i \rangle_b$). The heavy hole masses for the in-plane and z directions are calculated using the Luttinger-Kohn band parameters.

$$m_{h\parallel} = \frac{m_0}{\gamma_1 + \gamma_2}, \quad m_{h\perp} = \frac{m_0}{\gamma_1 - 2\gamma_2} \ . \tag{4}$$

We use the values $\gamma_1 = 5.15$, $\gamma_2 = 0.94$, and $m_e/m_0 = 0.079$ for the InP,[40] $\gamma_1 = 11.01$, $\gamma_2 = 4.18$, and $m_e/m_0 = 0.041$ for the $In_{0.53}Ga_{0.47}As$ (Ref. 41) material and a discontinuity distribution $\Delta E_C/\Delta E_V = \frac{35}{65}$.[42] The step height Δ and the lateral size Λ_{micro} are chosen according to the analysis of the PL linewidth ($\Delta = 1$ ML, $\Lambda_{micro} = 1.6$ nm).

In Fig. 7, the calculated ambipolar mobility [$\mu_{amb} = 2/(\mu_e^{-1} + \mu_h^{-1})$] is depicted versus temperature (dotted line). In good agreement with our experimental findings, the theoretical result shows a mobility nearly independent of temperature in the depicted temperature range for the parameters corresponding to our experiment.

If we notice the uncertainty in the determination of the lateral size Λ_{macro} of the macroislands from the cathodoluminescence measurements and the lateral size Λ_{micro} of the microroughness from the analysis of the luminescence linewidth, we find a good description of the experimental values by the theory of IRS in the temperature re-

gion between 60 and 130 K. We conclude that the roughness of the interface controls the exciton mobility as well as the luminescence linewidth in this quantum well. At lower temperatures, the influence of localized excitons is dominant, whereas at higher temperatures, our model should be modified, taking into account the thermal-induced transfer from the energetically lower (3 ML) to the energetically higher (2 ML) regions.

It should be noted that the ambipolar approximation used in our calculations is able to describe the excitonic mobilities very well. In the case of IRS, the scattering seems to be due to the specific characters of the electrons and the holes in the corresponding potential wells. Hence we do not expect a drastic change of the theoretical result, if we calculate the more complicated case of excitonic scattering.

Furthermore, we want to point out that the existence of a similar microroughness at both interfaces is only deduced from the HRTEM measurements. If we calculate the PL linewidth and the ambipolar mobility assuming a microroughness of $\Lambda_{\text{micro}}=2.6$ nm only at one interface, we get the same result as if we take the value of $\Lambda_{\text{micro}}=1.6$ nm for the microroughness at both interfaces. Hence, analyzing only the PL linewidth and the transfer dynamics, we cannot decide whether a certain microroughness is at both or only at one interface. However, we want to emphasize that a quantitative explanation of our experiments is not possible without the assumption of a microroughness either at one or at both interfaces.

V. SUMMARY

We have analyzed the exciton dynamics in thin $In_{0.53}Ga_{0.47}As/InP$ quantum wells prepared with growth interruption at each interface. Macroislands with an extension Λ_{macro} of around 1 μm cause a monolayer splitting in the excitonic emission.

The transfer between these extended islands is studied by means of time-resolved photoluminescence spectroscopy. At low temperatures exciton localization at potential fluctuations at the interfaces prevents the coupling between different island regions and causes an excitonic lifetime nearly independent of temperature. Increasing the temperature we find an effective interaction between the islands, and the exciton transfer modifies the luminescence decay of the quantum well.

A model including the diffusion in the islands and a transfer at the border of the islands is used for a quantitative description of our experiments. The deduced mobility reveals a gradual transition from exciton localization at low temperatures to interface roughness scattering limited exciton diffusion at temperatures between 60 and 130 K.

The quantitative value of the mobility as well as the additionally analyzed photoluminescence linewidth can only be understood by the assumption of some microroughness at the heterointerfaces. This microroughness has also been seen in high-resolution transmission electron microscopy and seems to be similar at both interfaces.

In conclusion, a consistent and quantitative description of the exciton dynamics in our structure is presented. The interface morphology (extended islands superimposed by a certain microroughness at one, only a microroughness at the other interface) controls the exciton transfer between the different island regions as well as the excitonic linewidth.

ACKNOWLEDGMENTS

We would like to thank A. Forchel and M. H. Pilkuhn for fruitful discussions. The financial support of the Deutsche Forschungsgemeinschaft under Contract No. SCHW 470/1-1 is gratefully acknowledged.

APPENDIX

By exciting the sample with a short laser pulse (pulse width much less than the recombination lifetime), the luminescence intensity of one region (2- or 3-ML areas) is given by the exciton population in this region, because the emission is caused by the recombination of excitons created by the low excitation intensities used in our experiments (we neglect nonradiative recombination processes). Assuming a cylinder geometry, we first calculate the temporal and spatial variation of the carrier concentration $c_{2\,\text{ML}}(r,t)$ in the 2-ML regions in consideration of the finite lifetime $\tau_{2\text{ML}}$ of the excitons, the excitonic diffusion in the islands and the transfer into the 3-ML regions at the border of the islands.

The following equations are used for a quantitative description of this problem:

$$\frac{\partial c_{2\,\text{ML}}(r,t)}{\partial t}=-\frac{c_{2\,\text{ML}}(r,t)}{\tau_{2\,\text{ML}}}+D\,\Delta c_{2\,\text{ML}}(r,t) \tag{A1}$$

including the surface condition

$$-\left.\frac{\partial c_{2\,\text{ML}}(r,t)}{\partial t}\right|_{r=\Lambda_{\text{macro}}/2}=S[c_{2\,\text{ML}}(r=\Lambda_{\text{macro}}/2,t)-c_{2\,\text{ML}}(r=\Lambda_{\text{macro}}/2,\ t=\infty)]\ . \tag{A2}$$

D corresponds to the excitonic diffusion constant, S denotes the transfer velocity at the border of the 2-ML islands, and Λ_{macro} is the diameter of the 2-ML islands. For $t\rightarrow\infty$, thermal equilibrium between the different islands is achieved.

The integral exciton population $C_{2\,\text{ML}}(t)$ in the 2-ML regions is then given by

$$C_{2\,\text{ML}}(t)=\int_0^{\Lambda_{\text{macro}}/2} dr\,2\pi r c_{2\,\text{ML}}(r,t)\ . \tag{A3}$$

The problem can be solved analytically and we get the following result:[43]

$$C_{2\,\mathrm{ML}}(t)=\left[C_\infty+\left[C_{20}-C_\infty\right]\sum_i\frac{4L^2\exp(-4\beta_i^2Dt/\Lambda_{\mathrm{macro}}^2)}{(\beta_i^2+L^2)\beta_i^2}\right]e^{-t/\tau_{2\,\mathrm{ML}}}, \tag{A4}$$

with the initial condition after δ pulse excitation $C_{20}=C_{2\,\mathrm{ML}}(t=0)$, the equilibrium condition $C_\infty=C_{2\,\mathrm{ML}}(t\to\infty)$ and the abbreviation $L=\Lambda_{\mathrm{macro}}S/2D$. The β_i's are given by the solution of

$$\beta_iJ_i(\beta_i)-LJ_0(\beta_i)=0\,, \tag{A5}$$

where $J_0(\beta_i)$ is the Bessel function of the first kind of order zero and $J_1(\beta_i)$ is the Bessel function of first order.

Using the solution for the carrier population in the 2-ML regions, it is possible to calculate the variation of the population $C_{3\,\mathrm{ML}}(t)$ in the 3-ML regions:

$$\frac{\partial C_{3\,\mathrm{ML}}(t)}{\partial t}=-\frac{C_{3\,\mathrm{ML}}(t)}{\tau_{3\,\mathrm{ML}}}+\frac{\partial C_t(t)}{\partial t}e^{-t/\tau_{2\,\mathrm{ML}}}. \tag{A6}$$

The first term describes the finite lifetime of the carriers in the 3-ML regions and the second part of Eq. (A6) corresponds to the transfer rate from the 2-ML regions into the 3-ML areas. $C_t(t)$ is given by

$$C_t(t)=C_\infty+\left[C_{20}-C_\infty\right]\sum_i\frac{4L^2\exp(-4\beta_i^2Dt/\Lambda_{\mathrm{macro}}^2)}{(\beta_i^2+L^2)\beta_i^2}\,. \tag{A7}$$

Equation (A6) can be solved analytically and the result is used to fit our experiments.

In first-order approximation, the ratio of the initial population $C_{2\,\mathrm{ML}}(t=0)/C_{3\,\mathrm{ML}}(t=0)$ after δ-pulselike excitation is given by the ratio $A_{2\,\mathrm{ML}}/A_{3\,\mathrm{ML}}$ of the island areas of the different regions. In this calculation, we only take into account the transfer from the 2-ML regions into the 3-ML regions. The thermal-induced repopulation of the 2-ML regions at higher temperatures as well as the thermal emission of the carriers into the InP barrier is neglected. So our model does not hold for temperatures above 130 K.

[1] A. Gold, Phys. Rev. B **38**, 10 798 (1989).
[2] H. Sakaki, T. Noda, K. Hirakawa, M. Tanaka, and T. Matsusue, Appl. Phys. Lett. **51**, 1934 (1987).
[3] H. Hillmer, A. Forchel, R. Sauer, and C. W. Tu, Phys. Rev. B **42**, 3220 (1990).
[4] J. Hegarty, K. Tai, and W. T. Tsang, Phys. Rev. B **38**, 7843 (1988).
[5] G. Bastard, C. Deladande, M. H. Meynadier, P. M. Frijlink, and M. Voos, Phys. Rev. B **29**, 7042 (1984).
[6] J. Singh, K. K. Bajaj, and S. Chaudhuri, Appl. Phys. Lett. **44**, 805 (1984).
[7] M. Tanaka and H. Sakaki, J. Cryst. Growth **81**, 153 (1987).
[8] C. W. Tu, R. C. Miller, B. A. Wilson, P. M. Petroff, T. D. Harris, R. F. Kopf, S. K. Sputz, and M. G. Lamont, J. Cryst. Growth **81**, 159 (1987).
[9] D. Bimberg, J. Christen, T. Fukunaga, H. Nakashima, D. E. Mars, and J. N. Miller, J. Vac. Sci. Technol. B **5**, 1191 (1987).
[10] T. Y. Wang, E. H. Reihlen, H. R. Jen, and G. B. Stringfellow, J. Appl. Phys. **66**, 5376 (1989).
[11] W. Seifert, J. O. Fornell, L. Ledebo, M. E. Pistol, and L. Samuelson, Appl. Phys. Lett. **56**, 1128 (1990).
[12] D. Grützmacher, K. Wolter, H. Jürgensen, and P. Balk, Appl. Phys. Lett. **52**, 872 (1988).
[13] H. Kamei and H. Hayashi, J. Cryst. Growth **107**, 567 (1991).
[14] D. Grützmacher, J. Cryst. Growth. **107**, 520 (1991).
[15] D. Bimberg, J. Christen, T. Fukunaga, H. Nakashima, D. E. Mars, and J. N. Miller, Superlatt. Microstruct. **4**, 257 (1988).
[16] S. Nilsson, A. Gustafsson, and L. Samuelson, Appl. Phys. Lett. **57**, 878 (1990).
[17] K. Streubel, F. Scholz, V. Härle, M. Bode, M. Grundmann, J. Christen, and D. Bimberg, in *Proceedings of the Third International Conference on InP and Related Materials* (IEEE, Piscataway, 1991), p. 468.
[18] B. Deveaud, T. C. Damen, J. Shah, and C. W. Tu, Appl. Phys. Lett. **51**, 828 (1987).
[19] F. Fujiwara, K. Kanamoto, and N. Tsukada, Phys. Rev. B **40**, 9698 (1989).
[20] M. Kohl, D. Heitmann, S. Tarucha, K. Leo, and K. Ploog, Phys. Rev. B **39**, 7736 (1989).
[21] K. Fujiwara, H. Katahama, K. Kanamoto, R. Cingolani, and K. Ploog, Phys. Rev. B **43**, 13 978 (1991).
[22] S. Nilsson, A. Gustafsson, X. Liu, L. Samuelson, M. E. Pistol, W. Seifert, J. O. Fornell, and L. Ledebo, Superlatt. Microstruct. **9**, 99 (1991).
[23] R. Sauer, S. Nilson, P. Roentgen, W. Heuberger, V. Graf, and A. Hangleiter, in *Proceedings of the 20th International Conference on the Physics of Semiconductors,* edited by E. M. Anastassakis and J. D. Joannopoulos (World Scientific, Singapore, 1990), Vol. 2, p. 1133.
[24] K. Streubel, V. Härle, F. Scholz, M. Bode, M. Grundmann, and J. Christen, J. Appl. Phys. (to be published).
[25] G. Bacher, H. Schweizer, J. Kovac, A. Forchel, H. Nickel, W. Schlapp, and R. Lösch, Phys. Rev. B **43**, 9312 (1990).
[26] J. Feldmann, G. Peter, E. O. Göbel, P. Dawson, K. Moore, C. Foxon, and R. J. Elliott, Phys. Rev. Lett. **59**, 2337 (1987).
[27] U. Cebulla, G. Bacher, A. Forchel, G. Mayer, and W. T. Tsang, Phys. Rev. B **39**, 6257 (1989).
[28] H. Hillmer, A. Forchel, S. Hansmann, M. Morohashi, E. Lopez, H. P. Meier, and K. Ploog, Phys. Rev. B **39**, 10 901 (1989).
[29] M. Gurioli, A. Vinattieri, M. Colocci, C. Deparis, J. Massies, G. Neu, A. Bosacchi, and S. Franchi, Phys. Rev. B **44**, 3115 (1991).
[30] T. Kuhn and G. Mahler, Solid-State Electron. **32**, 1851 (1988).
[31] M. Grundmann, J. Christen, K. Streubel, and F. Scholz (unpublished).

[32]J. Lee, H. N. Spector, and V. K. Arora, Appl. Phys. Lett. **42**, 363 (1983).
[33]J. A. Blum and G. Bastard, Solid State Commun. **53**, 727 (1985).
[34]B. Deveaud, B. Guenais, A. Poudoulec, A. Regreny, C.d'Anterroches, A. Ourmazd, and J. Cunningham, Phys. Rev. Lett. **65**, 2317 (1990).
[35]A. Ourmazd and J. Cunningham, Phys. Rev. Lett. **65**, 2318 (1990).
[36]A. Ourmazd, D. W. Taylor, J. Cunningham, and C. W. Tu, Phys. Rev. Lett. **62**, 933 (1989).
[37]C. A. Warwick, W. Y. Jan, and A. Ourmazd, Appl. Phys. Lett. **56**, 2666 (1990).
[38]M. Sugawara, T. Fujii, S. Yamazaki, and K. Nakajima, Phys. Rev. B **42**, 9587 (1990).
[39]M. Grundmann and D. Bimberg, Phys. Rev. B **38**, 13 486 (1988).
[40]*Physics of Group IV Elements and III-V Compounds,* edited by O. Madelung, Landolt Börnstein, New Series, Vol. 17, Pt. a (Springer, Berlin, 1982).
[41]K. Alavi, R. L. Aggarwal, and S. H. Groves, Phys. Rev. B **21**, 1311 (1980).
[42]R. E. Cavicchi, D. V. Lang, D. Gershoni, A. M. Sergent, J. M. Vandenberg, S. N. G. Chu, and M. B. Panish, Appl. Phys. Lett. **54**, 749 (1989).
[43]J. Crank, *The Mathematics of Diffusion* (Clarendon Oxford, 1975), p. 79.